2019 SECED Conference
Earthquake risk and engineering towards a resilient world
9-10 September 2019, Greenwich, London

FAULT REACTIVATION VIA PRE-EXISTING FRACTURE NETWORKS DURING HYDRAULIC FRACTURING

James VERDON[1], Nadine IGONIN[2], Michael KENDALL[2], David EATON[1]

Abstract: *Developing an improved understanding of the mechanisms by which hydraulic fracturing causes induced seismicity is vital if we are to mitigate the occurrence of such events. In this paper we present data from a case study in Alberta, Canada, where events exceeding magnitude M_W = 3 were recorded. Our monitoring recorded over 18,000 microseismic events, which revealed the presence of pre-existing fracture corridors that intersect the treatment wells. These fracture corridors are instrumental in facilitating the transfer of elevated fluid pressures towards larger faults on which the largest seismic events occurred. In showing this effect, this study demonstrates the importance of understanding the hydrogeological conditions in a shale body, and in particular the presence of permeable fracture networks, when assessing potential seismic hazard associated with hydraulic fracturing.*

It is now widely accepted that hydraulic fracturing for shale gas has caused induced seismic activity (e.g., Bao and Eaton, 2016). Several instances with induced events with M > 4 have been identified in the Western Canadian Sedimentary Basin (Kao et al., 2018), while notable cases of hydraulic fracturing-induced seismicity have also been occurred in North America (Skoumal et al., 2015) and China (Meng et al., 2019).

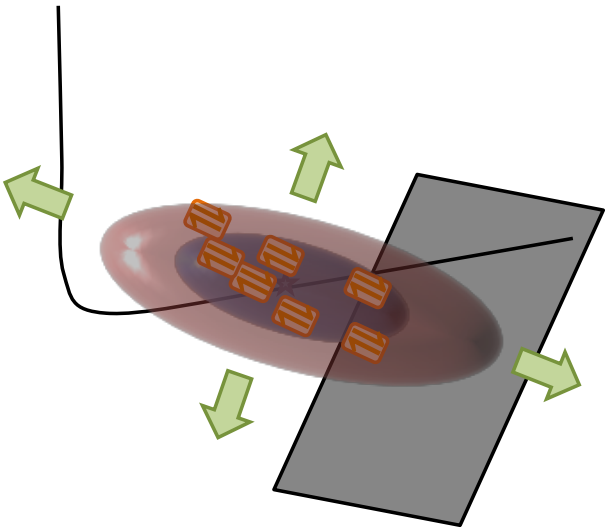

Figure 1. Schematic depiction of the various mechanisms by which hydraulic fracturing may cause fault reactivation. The fault may be invaded by the pressurised fracturing fluid itself (blue ellipsoid), or by the pore fluid pressure pulse that will propagate in advance of the fluid front (red ellipsoid). Alternatively, the increase in pore pressure (green arrows) and opening of fractures (orange squares) will impart poroelastic stresses into the rock frame that cause reactivation.

The causative mechanisms for such events is often not well constrained (Figure 1). The elevated pore pressures associated with hydraulic fracturing are an obvious candidate, as these reduce normal stresses on a fault, allowing slip to occur. However, the low permeability of shale limits the distances to which such pressure changes could propagate. Observations of seismicity at larger distances have led some to suggest poroelastic stress transfer through the rock frame itself as an alternative causative mechanism (e.g. Deng et al., 2016).

We study the Tony Creek dual Microseismic Experiment (ToC2ME) from the Duvernay Shale, Alberta (Eaton et al., 2018). The Duvernay is a tight shale with permeabilities c. 10^{-3} mD. Hydraulic

[1] University of Bristol, Bristol, UK. James.Verdon@bristol.ac.uk
[2] University of Calgary, Calgary, Canada.

fracturing at this site was conducted over multiple stages in 4 horizontal wells (Figure 2). Well C was the first well to be stimulated along its entire length, after which Wells A, B and D were stimulated in a "zipper-frac" system. The site was monitored with a near-surface array of 70 instrumented shallow boreholes, each of which was drilled to 20 m depth and contained 3 1-component geophones and 1 3-component geophone. We used a beamforming algorithm (Verdon et al., 2017) to detect and locate a catalogue of 18,000 microseismic events (Figure 2).

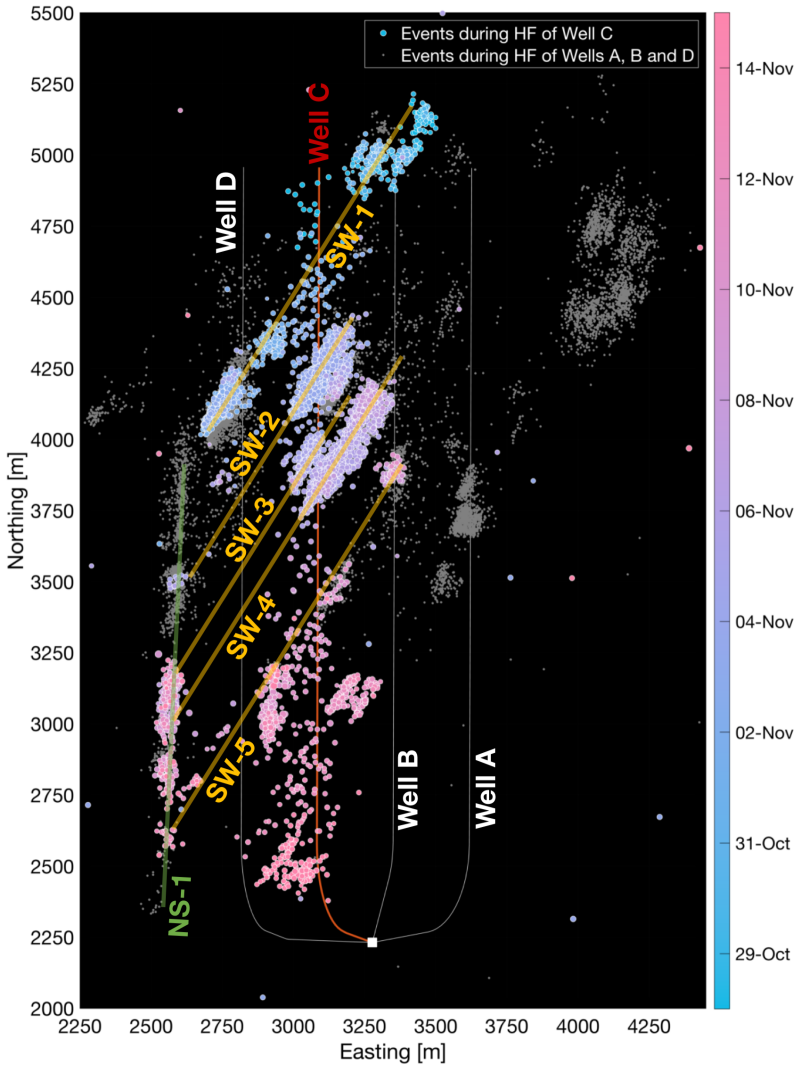

Figure 2. Map of events recorded during hydraulic fracturing at the ToC2ME site. Events during Well C stimulation are shown with larger, coloured symbols. Later events that occurred during stimulation of Wells A, B and D are shown by the grey dots. Five south-west trending event clusters are highlighted, which connect to the NS-1 feature to the west of the wells on which the largest seismic events occurred.

We focus on events that occurred during stimulation of Well C, noting 2 key features revealed by the event locations. Firstly, there is a linear feature roughly 1.5 km long extending with a roughly N-S orientation to the west of Well D. The largest events in the sequence, with magnitudes M_W > 3, occurred along this feature. We infer that this feature is a pre-existing strike-slip fault that was reactivated by the hydraulic fracturing. We term this feature NS-1. The focus of our study is on understanding how hydraulic fracturing in Well C causes the reactivation of NS-1, which is roughly 600 m distance from the well.

Secondly, there are several NE-SW-trending lineaments that intersect Well C. These clusters have lower magnitudes (M_W < 1), and *b* values of c. 2 (Igonin et al., 2018). We infer that these features are pre-existing fracture networks. We term these features SW-1 to SW-5, from north to south.

The spatio-temporal evolution of the seismicity is of particular significance (Figure 3). As hydraulic fracturing proceeds along Well C, each of the SW-1 to SW-5 features is activated when it is reached by the stimulation. The NS-1 fault is activated after the activation of the SW-2 feature. The first events on the NS-1 fault occur in direct alignment with SW-2, i.e. where SW-2 and NS-1 intersect. The next phase of seismicity on the NS-1 fault occurs in direct alignment with SW-3, where this feature intersects NS-1. This pattern is repeated for the SW-4 and SW-5 clusters – these features are activated directly by the hydraulic fracturing in Well C, and subsequently seismicity occurs on the NS-1 fault at locations that are in alignment with the SW trending clusters.

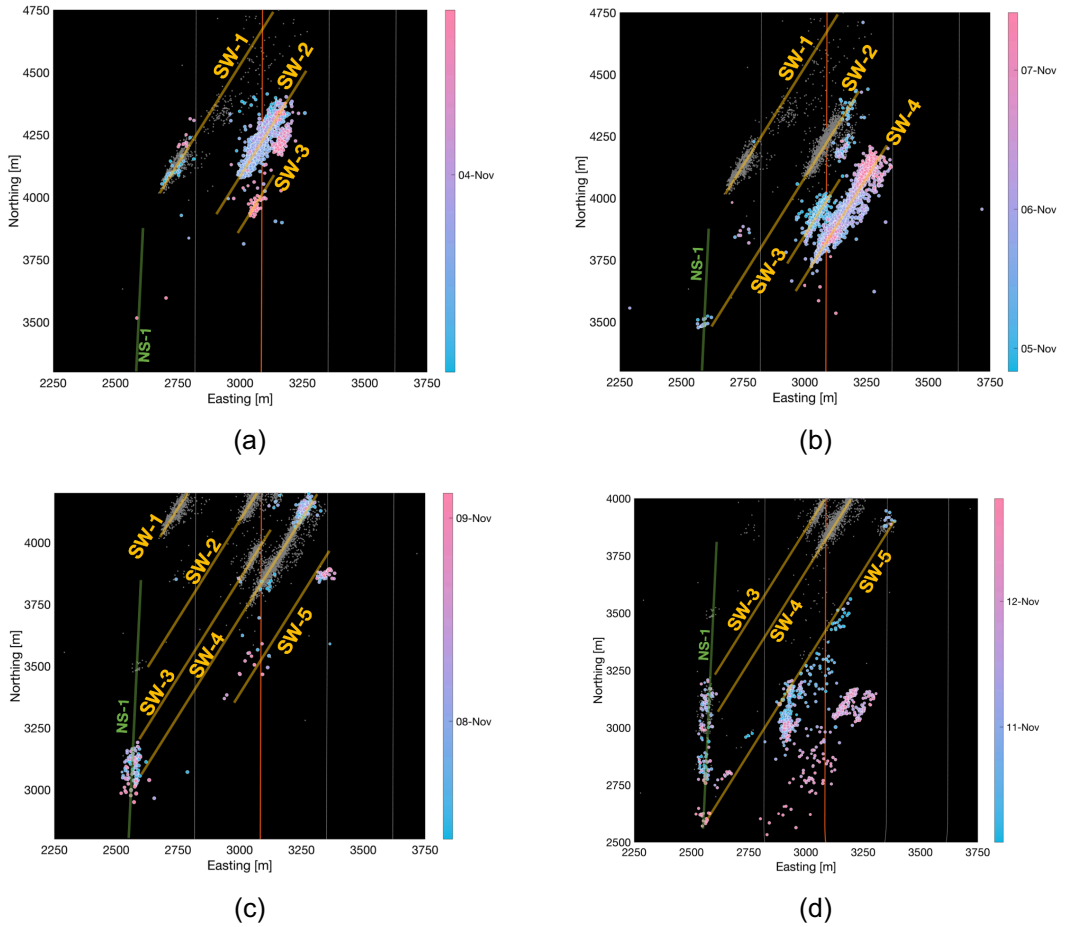

Figure 3. Temporal evolution of the ToC2ME seismicity. Coloured dots show the events that occurred during each time window, and grey dots show events that occurred prior to this time. In (a), SW-1 was active as the stimulation moved past this zone, after which the activity ceased. SW-2 was active, and SW-3 was beginning to activate. In (b), we see the first activity on the NS-1 fault. The location of this activity is aligned with the strike of SW-2 (i.e. where this feature would intersect NS-1). SW-4 has become active at this time as stimulation is moved southwards along the well. In (c), the next phase of reactivation occurs on the NS-1 feature. The location of this activity is aligned with the intersection of the SW-3 and SW-4 features. The SW-5 cluster has just begin to activate as stimulation moves further southwards. In (d) we see the onset of seismicity on NS-1 that is aligned with the strike of the SW-5 feature.

Our interpretation is therefore that the SW fracture corridors are providing a conduit for fluid flow, transferring elevated pressures from the stimulated zone to the NS-1 fault. Table 1 lists the time delay between activation of each SW cluster and the occurrence of seismicity on the corresponding portion of the NS-1 fault. This time delay ranges between 40 – 100 hours. Fluid flow modelling shows that this time lag is consistent with a fracture network having a permeability of roughly 100 – 200 mD.

Cluster	Date/Time activated at the well	Date/Time activation on corresponding part of NS-1	Time Delay (hours)
SW-2	Nov 2nd, 23:00	Nov 4th, 20:00	44
SW-3	Nov 4th, 18:00	Nov 7th, 10:00	64
SW-4	Nov 5th, 07:00	Nov 9th, 03:00	92
SW-5	Nov 8th, 18:00	Nov 12th, 20:00	98

Table 1. Delay times between the reactivation of each SW cluster, and the onset of seismic activity on corresponding portion of the NS-1 fault

Our observations and interpretations show the importance of pre-existing fracture networks in contributing to induced seismicity during hydraulic fracture stimulation. The larger the distance affected by the stimulation, the greater the probability that a pre-existing critically stressed fault will be encountered. However, the low permeability of shale limits the distance to which elevated pore pressures can typically propagate from the well. In this case study, the presence of pre-existing fracture corridors provided a pathway along which elevated pore fluid pressures were transferred to a fault, leading to reactivation. This fault would not have been reached from Well C (at a distance of c. 600 m) without the presence of these fractures, as evidenced from the fact that the Well C stages that did not interact with the SW-trending fracture corridors did not produce activation on the NS-1 fault.

Acknowledgements

Financial support was provided by Chevron and the Natural Sciences and Engineering Research Council of Canada (NSERC) through the NSERC-Chevron Industrial Research Chair in Microseismic System Dynamics. Continuous geophone data were recorded under license from Microseismic Inc. for use of the BuriedArray method.

References

Bao X and Eaton DW (2016), Fault activation by hydraulic fracturing in Western Canada, *Science* 354, 1406-1409.

Deng K, Liu Y, Harrington RM (2016), Poroelastic stress triggering of the December 2013 Crooked Lake, Alberta, induced seismicity sequence, *Geophysical Research Letters* 43, 8482-8491.

Eaton DW, Igonin N, Poulin A, Weir R, Zhang H, Pellegrino S, Rodriguez G, (2018), Induced seismicity characterisation during hydraulic fracture monitoring with a shallow-wellbore geophone array and broadband sensors, *Seismological Research Letters* 89, 1641-1651.

Igonin N, Zecevic M, Eaton DW (2018), Bi-linear magnitude-frequency distributions and characteristic earthquakes during hydraulic fracturing, *Geophysical Research Letters* 45, 12866-12874.

Kao H, Visser R, Smith B, Venables S (2018), Performance assessment of the induced seismicity traffic light protocol for northeastern British Columbia and western Alberta, *The Leading Edge* 37, 117-126.

Meng L, McGarr A, Zhou L, Zang Y, (2019), An investigation of seismicity induced by hydraulic fracturing in the Sichuan Basin of China based on data from a temporary seismic network, *Bulletin of the Seismological Society of America* 109, 348-357.

Skoumal RJ, Brudzinski MR, Currie BS (2015), Induced earth-quakes during hydraulic fracturing in Poland Township, Ohio, *Bulletin of the Seismological Society of America* 105, 189-197.

Verdon JP, Kendall JM, Hicks SP, Hill P, (2017), Using beamforming to maximise the detection capability of small, sparse seismometer arrays deployed to monitor oil field activities, *Geophysical Prospecting* 65, 1582-1596

Zhang H, Eaton DW, Rodriguez G, Jia S, (2019), Source-mechanism analysis and stress inversion for hydraulic-fracturing-induced event sequences near Fox Creek, Alberta, *Bulletin of the Seismological Society of America* 109, 636-651.